GUFBD / *GUJS* (2022) 12(2): 487-497
DOI: 10.17714/gumusfenbil.1008242 Araştırma Makalesi / *Research Article*

Monitoring burn severity and air pollutants in wildfire events using remote sensing data: the case of Mersin wildfires in summer 2021

Uzaktan algılama verileri ile orman yangınlarında yanma şiddetinin ve hava kirleticilerinin izlenmesi: 2021 yazı Mersin orman yangınları örneği

Muzaffer Can İBAN*[1,a], Ezgi ŞAHİN[2,b]
[1]Mersin Üniversitesi, Mühendislik Fakültesi, Harita Mühendisliği Bölümü, 33343, Mersin
[2] Mersin Üniversitesi, Fen Bilimleri Enstitüsü, Uzaktan Algılama ve Coğrafi Bilgi Sistemleri Programı, 33343, Mersin

• Geliş tarihi / *Received*: 12.10.2021 • Düzeltilerek geliş tarihi / *Received in revised form*: 31.01.2022 • Kabul tarihi / *Accepted*: 08.02.2022

Abstract
Remotely sensed data have been used to investigate air pollutants and matter toxicity, land cover changes and burn severity. The goal of this study is to analyze land and atmospheric data for wildfire events that occurred in Mersin Province between July 28 and August 3, 2021. We used a variety of open-access remotely sensed data sets (MODIS, Sentinel 2A and Sentinel 5P TROPOMI) from the pre-fire (20-27 July), fire (28 July – 3 August), and post-fire period (4-10 August). This comprehensive study's findings can be divided into two categories. The first group is the land cover output, which includes maps of the affected region's land surface temperature and burn severity, as well as comparisons of the two. The atmospheric output, which consists of trace gas column density maps (for carbon monoxide, formaldehyde, sulphur dioxide and ozone), is the second group. The quantitative results of these analyses indicate that high severity areas correspond to 16.536 hectares, and the maximum column number density reached to 0.071 mol/m^2 for carbon monoxide, 0.0043 mol/m^2 for formaldehyde, 0.00049 mol/m^2 for sulphure dioxide and 0.137 mol/m^2 for ozone. The burn severity is found to be highly correlated with land surface temperatures. Pollutant levels in the atmosphere were found to be rising during and after the wildfire. There has not been any evidence of a significant increase in air pollutants near urban areas. However, ozone concentrations rose significantly after the wildfire because the province's nitrogen oxide levels were high enough to produce ozone.

Keywords: Air pollutants, Burn severity index, Land surface temperature, Sentinel-5P, Wildfires

Öz
Hava kirleticilerini, madde zehirliliğini, arazi örtüsü değişimini ve yanma şiddetini izlemek için uzaktan algılama verilerinden faydalanan çalışmalar yapılmaktadır. Bu çalışmanın amacı, Mersin İli'nde 28 Temmuz – 3 Ağustos 2021 tarihleri arasında gerçekleşen orman yangınları sonucunda gözlemlenen arazi örtüsü ve atmosfer verilerini analiz etmektir. Yangın öncesi (20-27 Temmuz), yangın (28 Temmuz-3 Ağustos) ve yangın sonrası (4-10 Ağustos) dönemleri için çeşitli açık erişimli uzaktan algılama verileri (MODIS, Sentinel 2A ve Sentinel 5P) kullanılan bu çalışmanın bulguları iki kategoride belirtilebilir. İlk kategori, etkilenen bölgenin arazi yüzey sıcaklığı ve yanık şiddeti haritalarının hazırlanmasını ve bunların arasındaki ilişkinin karşılaştırılmasını içermektedir. İkinci kategori ise, kirletici gazların (karbon monoksit, formaldehit, sülfür dioksit ve ozon) düşey yoğunluk haritalarını içeren atmosferik çıktılardır. Bu analizlerin nicel sonuçları, yüksek şiddetli yanma alanlarının 16.536 hektara karşılık geldiğini ve maksimum düşey molekül yoğunluğunun karbon monoksit için 0.071 mol/m^2, formaldehit için 0.0043 mol/m^2, kükürt dioksit için 0.00049 mol/m^2 ve ozon için 0.137 mol/m^2'ye ulaştığını göstermektedir. Yanma şiddetinin, arazi yüzey sıcaklıkları ile yüksek oranda ilişkili olduğu saptanmıştır. Orman yangını sırasında ve sonrasında atmosferdeki kirletici seviyelerinin yükseldiğini tespit eden bu çalışma, kentsel alanların yakınında hava kirleticilerinde önemli bir artış olduğuna dair herhangi bir kanıt bulamamıştır. Ancak, ozon gazı yoğunluğunun orman yangınından sonra, il genelindeki yüksek nitrojen oksit seviyesine bağlı olarak önemli ölçüde yükseliş gösterdiği gözlemlenmiştir.

***Anahtar kelimeler**: Hava kirleticileri, Yanma şiddeti endeksi, Arazi yüzeyi sıcaklığı, Sentinel-5P, Orman yangınları*

[*a] Muzaffer Can İBAN; caniban@mersin.edu.tr, Tel: (0324) 361 00 01, orcid.org/0000-0002-3341-1338
[b] orcid.org/0000-0002-7455- 8141

1. Introduction
1.Giriş

Wildfires have taken the great attention of scholars due to their dire consequences on forests and sustainable land use, especially in the Mediterranean countries. Wildfires, in simple terms, destroy the vegetated land cover and diminish the amount of fertile land because of land erosion and loss of fundamental nutrients in the ecosystem (Fernández et al., 2007; Magro et al., 2021). In terms of land management and public administration, the wildfires create a huge risk for peri-urban settlements and houses are important assets to prevent the devastating effects of wildfires. Policymakers must recognize that global warming has a direct impact on fire severity, and they must take steps to reduce the risks of future wildfires. (Lindenmayer et al., 2020).

Turkey is one of the Mediterranean countries afflicted by destructive wildfires. Turkey faced the worst and most devastating wildfires in its history in July and August 2021. This series of wildfires was particularly effective on the southern coasts (Muğla, Antalya, and Mersin provinces), and it is estimated that 170,000 hectares of rural lands were exposed to wildfires during this period (Fu, 2022). The start of wildfires coincides with the region's high-temperature records.

Several studies have been conducted using remote sensing products to investigate the post-disaster effects of wildfires. Examples include atmospheric studies on air pollutants and matter toxicity (Langmann et al., 2009; Wu et al., 2006) or land cover changes (Chuvieco & Congalton, 1989; Eva & Lambin, 2000) and burn severity (Cocke et al., 2005; Keeley, 2009). Researchers can use remote sensing data to detect changes in vegetation after wildfires, as well as monitor the area affected by wildfires and the ecosystem dynamics when the affected area regenerates. Spectral indices (for example, Normalized Difference Vegetation Index – NDVI or Normalized Burn Ratio – NBR) aid in tracking the severity of wildfires as well as the rate of vegetation enhancement in affected areas. Scholars have used these indices for previous wildfires in Kahramanmaraş (Dindaroglu et al., 2021), İzmir (Çolak & Sunar, 2020; Nasery & Kalkan, 2020; Sabuncu & Özener, 2019) and Mersin provinces (Tonbul et al., 2016). All of these studies contributed important findings to the existing body of literature on land management and disaster recovery. Using remotely sensed data sets, however, atmospheric trends of carbon dioxide, sulphur dioxide, formaldehyde, and ozone from wildfires were tracked for Portugal (Magro et al., 2021), Ukraine (Savenets et al., 2020), California (Schneising et al., 2020) and Canada (Alvarado et al., 2020). These case studies provided compelling evidence for the use of remote sensing to track the spatial and temporal patterns of atmospheric trace gases in the aftermath of a major wildfire. A preliminary air quality assessment of recent wildfires in Turkey was conducted for the provinces of Antalya and Muğla, revealing that the wildfires this season have significantly reduced air quality in the region (Salman et al., 2021).

There are not too many case studies in the literature that cover both fire severity and atmospheric trace gas tracking simultaneously. The objective of this research is to conduct a combination of land and atmospheric data analysis for wildfire events that occurred in Mersin Province between July 28 and August 3, 2021. To do so, we used a variety of open-access remotely sensed data sets from the pre-fire (20-27 July), fire (28 July – 3 August), and post-fire periods (4-10 August). Section 2 introduces the site description and data sets used. As shown in Section 3, the findings of this comprehensive study can be divided into two categories. The first group is the land cover output, which includes the affected region's land surface temperature and burn severity maps, as well as their comparison. The second group is the atmospheric output, which consists of trace gas column density maps. All of the maps were created to understand the individual or inter-dependent dynamics of trace gases during the extreme wildfire event in Mersin Province.

2. Materials and methods
2. Materyaller ve metotlar

2.1. Site description
2.1. Çalışma alanı

This study was carried out in Mersin Province (Figure 1), with a particular focus on Aydıncık district and Yeşilovacık villages in the province's western part. Mersin Province is located on the Mediterranean coast in southern Turkey. The district of Aydıncık is an urban settlement (circa 11 thousand inhabitants); however, other nearby urban areas to the wildfire zone are the districts of Silifke (circa 125 thousand inhabitants) and Gülnar (circa 20 thousand inhabitants). The study area includes maquis, garrigue (sage, rosemary, thyme, lavender), and sandy areas near the seashore. *Pinus brutia* is a dominant tree species in the monitored area's forests.

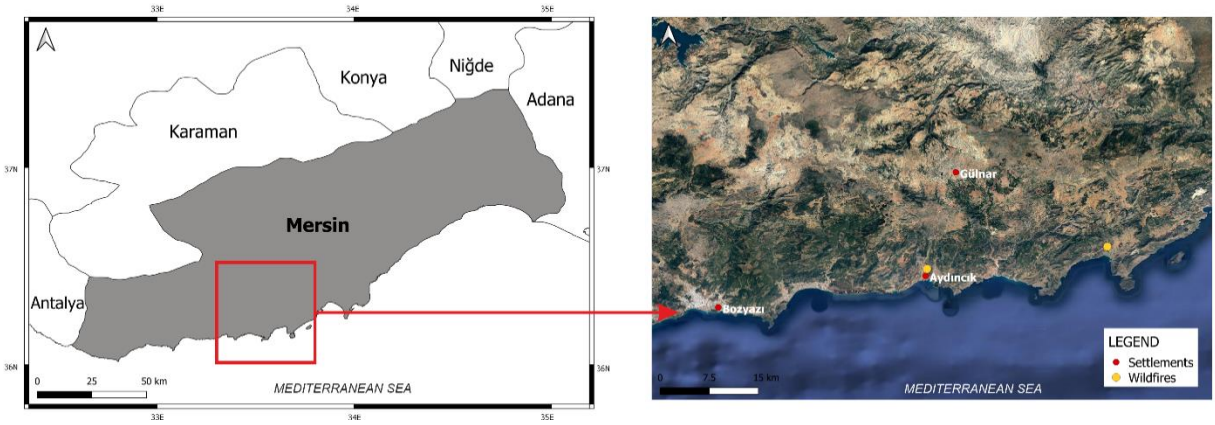

Figure 1. Study area with a focus on affected zone
Şekil 1. *Etkilenen alana odaklı çalışma sahası*

2.2. Land data sets
2.2. Arazi veri setleri

2.2.1. Land surface temperature
2.2.1. Arazi yüzeyi sıcaklığı

Land Surface Temperature (LST) is an important component of the physical Earth because it allows us to understand the energy interactions between the atmosphere and land. The LST data set has been used in a variety of studies, including climate change, hydrology, and ecological assessment (Bao et al., 2011). The MOD11A1 LST product from the Moderate-resolution Imaging Spectroradiometer (MODIS) instrument, with a spatial resolution of 1 km and a temperature resolution of 0.02 Kelvin, is one of the resources for retrieving LST images. Each LST image is created by analyzing the emitted thermal-infrared radiance values in two spectral bands (11.00 and 12.02 mm) (Imhoff et al., 2010). This image processing employs a radiance-based split-window algorithm, which allows us to compute the relationship between radiance and temperature using a radiative transfer function (Wang et al., 2019). When compared to in-situ measurements, the MOD11A1 LST product has a positional accuracy of 50 meters and a temperature accuracy of less than 0.5 Kelvin (Wolfe et al., 2002). MOD11A1 signals cannot penetrate clouds; thus, LST images can be retrieved as long as the sky is clear and the temperature radiance of the top of the clouds is not mixed with the land surface. Another advantage of MOD11A1 products is that due to MODIS' ascending and descending orbits, LST images can be retrieved both during the day and at night. (Wan et al., 2004).

In this study, LST images obtained at night from the MOD11A1 product were examined for pre-fire, fire, and post-fire periods in order to detect the magnitude of temperature rise on bare land surface caused by recent wildfires. Google Earth Engine (GEE) was used to download the LST image composites for three different time periods. The GEE platform includes algorithms for creating composite images for specific time periods; as a result, GEE allows for faster image acquisition rather than downloading single image files from NASA servers (Ebrahimy et al., 2021). LST images for the daytime were excluded from this study because the study area is extremely hot in the summer, and variations in LST cannot be detected because the hot weather warms the land surface significantly.

2.2.2. Burn area detection and burn severity
2.2.2. Yanmış alan tespiti ve yanma şiddeti

Remotely sensed data sets are pioneer tools for monitoring, analyzing, and administering burnt forests on a global or regional scale, as they enable rapid monitoring over burnt areas for mitigating post-fire effects (Llorens et al., 2021). In comparison to manual delineation or in-situ observations, remote sensing approaches have provided higher accuracies for detecting the burnt area. Furthermore, researchers can characterize burn severity patterns using remote sensing techniques (Fassnacht et al., 2021).

Burn severity, by definition, corresponds to the long-term land cover and ecological changes of an affected area and allows for the measurement of the landscape's responses after a wildfire. Tree mortality, vegetation enhancement, and recolonization are examples of these responses (Cansler & McKenzie, 2012; Keeley, 2009). An index known as the differenced Normalized Burn Ratio (dNBR) has become a popular method for determining burn severity. By combining the near infrared (NIR) and shortwave infrared (SWIR)

wavelengths of any multispectral sensor, it highlights the burned lands. Healthy vegetation has significantly higher reflectance values in NIR portion of the electromagnetic spectrum, while it has lower reflectance in the SWIR. The areas devastated by a wildfire, on the other hand, exhibit the inverse trend. As a result, the difference in spectral differences between healthy and burned landscapes reaches the top in both the NIR and SWIR portions. (Díaz-Delgado et al., 2003).

In this study, we computed dNBR using Sentinel-2 Level-2A composite images with a spatial resolution of 20 meters derived from GEE. Atmospherically corrected surface reflectance is shown in Level-2A images; thus, there was no need for atmospheric correction. The pre-fire image composite is made up of cloudless image tiles in between May 1 and July 27, while the post-fire image composite is made up with image tiles between July 28 and October 1. We calculated dNBR on GEE with the following equations, using Band 8A (NIR – 864.8 nm) and Band 12 (SWIR – 2202.4 nm).

$$NBR = (NIR - SWIR) / (NIR + SWIR) \quad (1)$$

$$dNBR = NBR_{pre\text{-}fire} + NBR_{post\text{-}fire} \quad (2)$$

where dNBR is computed using the Normalized Burn Ratios (NBR) of pre-fire and post-fire composite images. The greater the value of dNBR, the more severe the damage in the affected area. These damages are classified using pre-defined intervals proposed by the USGS (Key & Benson, 2006), as seen in Table 1. Sub-zero dNBR values correspond to increased vegetation regrowth in the affected area.

Table 1. Severity intervals used in dNBR analysis
Tablo 1. *dNBR analizinde kullanılan şiddet aralıkları*

Severity Level	dNBR Range
Enhanced Regrowth, high (post-fire)	-0.500 to -0.251
Enhanced Regrowth, low (post-fire)	-0.250 to -0.101
Unburned	-0.100 to +0.99
Low Severity	+0.100 to +0.269
Moderate-low Severity	+0.270 to +0.439
Moderate-high Severity	+0.440 to +0.659
High Severity	+0.660 to +1.300

2.3. Air pollutants data sets
2.3. Hava kirleticileri veri setleri

Wildfires produce a large amount of trace gases, which have a significant impact on the chemical composition of the atmosphere and climate. Because of wood combustion, wildfire smoke emits a variety of pollutants, including carbon monoxide (CO), formaldehyde (HCHO), and sulphur dioxide (SO_2) (Magro et al., 2021) Furthermore, wildfires produce tropospheric ozone (O_3), which has a negative impact on ecosystems; thus, it is important to monitor O_3 levels after a wildfire.

CO is a colorless, odorless, and tasteless chemical gas that degrades atmospheric air quality. It has the potential to cause serious health problems when inhaled by living species because it can disrupt the transport of oxygen through the veins (Omaye, 2002). Smoke from wildfires may reach human settlements, prompting health officials to advise residents to stay indoors. This smoke evidently contains CO, which is produced by the incomplete combustion of burning biomass materials in wildfire areas. Several remote sensing instruments were used by the researchers to monitor CO. (Schneising et al., 2020). Formaldehyde (HCHO) is one of the most common non-methane volatile organic compounds emitted by wildfires. This aldehyde's emission varies with carbon emissions depending on fuel type and combustion efficiency; thus, HCHO is more available in smoldering wildfires. (Liu et al., 2017). HCHO is known to be a respiratory carcinogen, and excessive HCHO exposure significantly increases the risk of asthma and cancer (National Toxicology Program, 2010). According to some research, wildfires emit higher HCHO concentrations than normal conditions; thus, it is critical to monitor HCHO levels in the atmosphere during and after a devastating wildfire (Na & Cocker, 2008). Sulphur naturally occurs in nature, but when it comes into contact with combustible conditions, it transforms into sulphuric acid and sulphur dioxide (SO_2) in the air. Acid rain is caused by sulphuric acid. SO_2 concentrations above a certain threshold cause respiratory and cardiovascular diseases in living organisms. (Aryal et al., 2018). Sulphur dioxide (SO_2), one of the pollutants in wildfire smoke, is particularly toxic to plants in close proximity to wildfires, causing protein degradation and cell death (Weber et al., 2021). Because SO_2 dispersion is highly dependent on wind speed and direction; the SO_2 maps must be compared to meteorological data. O_3 is well-known as a second-level air pollutant that causes a variety of respiratory diseases. O_3 is formed by the chemical interaction of nitrogen oxides and organic carbons in the presence of sunlight. Wildfires also emit significant amounts of O_3 precursors, and the ratios increase downwind of a wildfire (Watson et al., 2019). O_3 production is highly correlated with the

amount of nitrogen oxides (NO_x); in other words, when NO_x levels are high, O_3 production may decrease. (McClure & Jaffe, 2018).

In this study, we used column number density data of CO, HCHO, SO_2, and O_3 at ground level from the TROPOspheric Monitoring Instrument (TROPOMI) on the European Space Agency's Sentinel-5 Precursor (S5P) satellite. Many scholars have used and recommended TROPOMI data for air pollution monitoring (Kaplan & Yigit Avdan, 2020). S5P measures CO global abundance using clear-sky and cloudy-sky Earth radiance measurements in the 2.3 m spectral range of the solar spectrum's shortwave infrared (SWIR). TROPOMI, which provides excellent SO_2 and HCHO images with a low signal-to-noise ratio, can be used to observe tropospheric SO_2 and HCHO column number density. TROPOMI also provides offline O_3 images via the GODFIT algorithm. The spatial resolution of all of the data sets provided is 1113.2 meters. (TROPOMI, 2021).

3. Results and discussion
3. Bulgular ve tartışma

Figure 2 shows LST images at night derived from the MOD11A1 product. Pre-fire, fire, and post-fire LST composite maps were created separately. Temperature differences between periods are significant, and the spatial variability of LST can be visually distinguished between burnt and unburnt zones. The mean LST in burnt areas during the pre-fire period was 24.1 °C, 32.9 °C during the fire period, and 29.8 °C in the post- fire period, according to numerical results derived from pixel values.

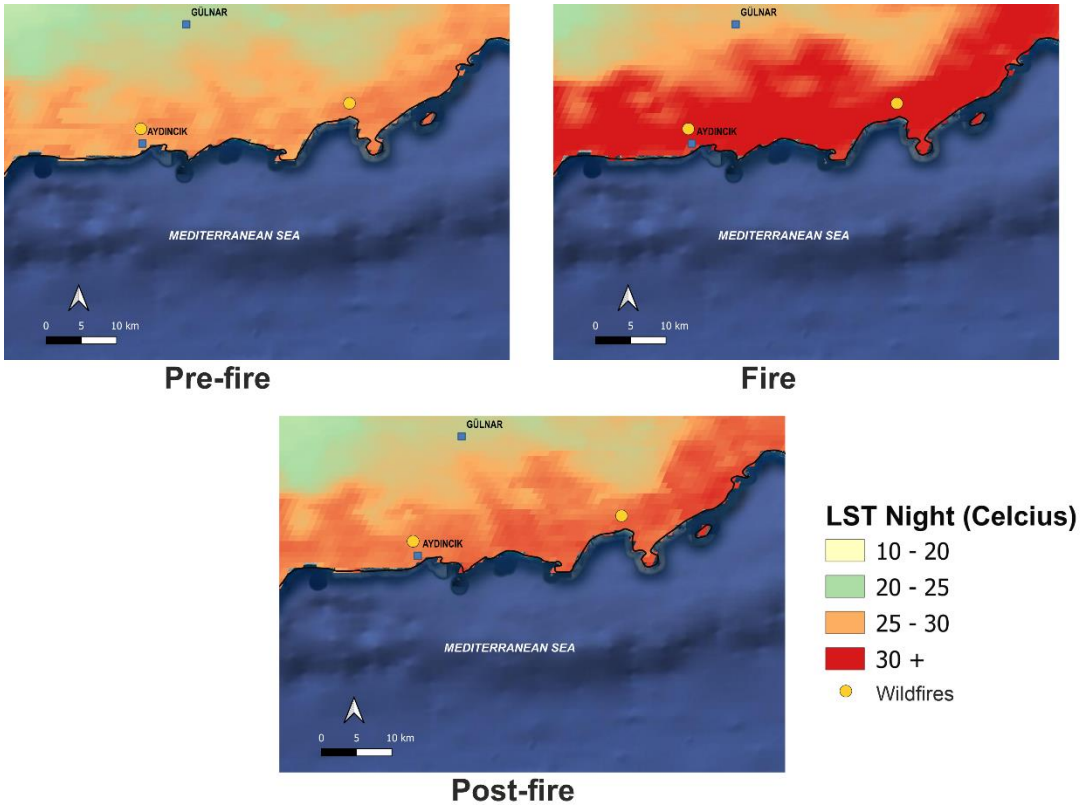

Figure 2. Pre-fire, fire, and post-fire LST maps for the affected zone
Şekil 2. *Etkilenen bölgenin yangın öncesi, yangın esnasında ve yangın sonrası LST haritaları*

Figure 3 depicts a dNBR-based burn severity map generated for the affected zone. The affected zone has low severity areas of 190.812 hectares, moderate-low severity areas of 163.42 hectares, moderate-high severity areas of 88.792 hectares, and high severity areas of 16.536 hectares, according to pixel statistics computed in QGIS raster processing toolbox.

Several studies have discovered a relationship between post-fire LST and burn severity maps derived from satellite imagery (Çolak & Sunar, 2020). As a result, we investigated the relationship between dNBR values and LST values of stratified sampled 83 pixels on the affected zone. The second order polynomial regression plots in Figure 4 show a strong positive correlation between dNBR values and LST values of both the fire (Pearson's

Correlation Coefficient = 0.870) and post-fire periods (Pearson's Correlation Coefficient = 0.856), which supports the findings of previous studies. In other words, the higher the land temperature in our study area, the more severe the burn severity of the vegetation exposed to. Because our post-fire image composite spans the period until October 2021, we can conclude that there has been no enhanced regrowth of vegetation in the affected zone thus far.

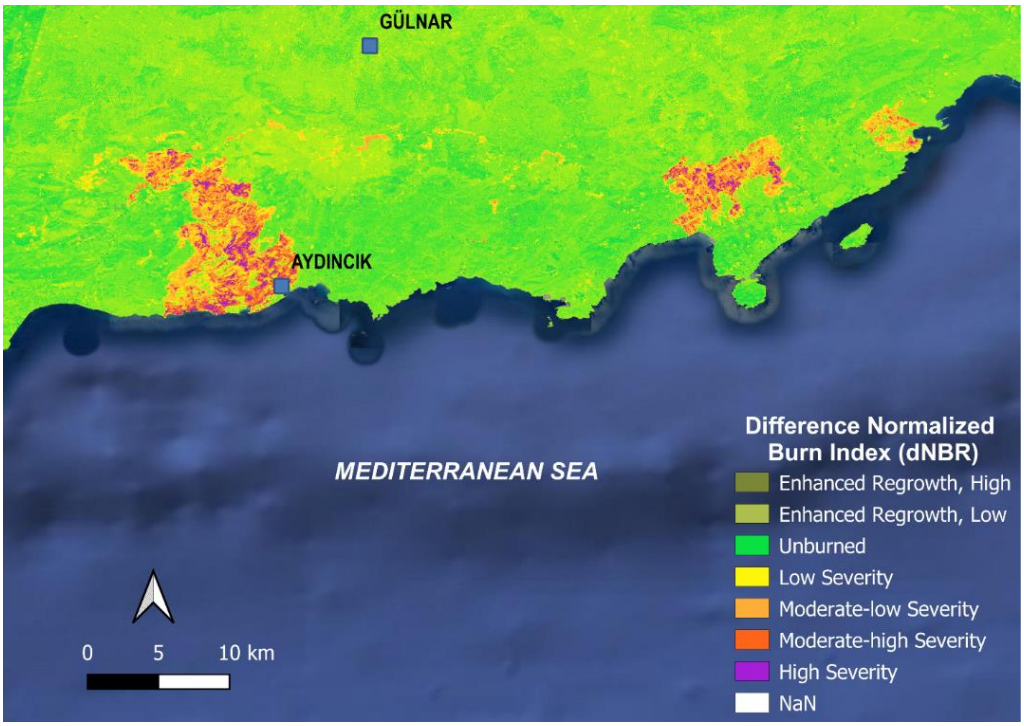

Figure 3. Burn severity map based on dNBR generated from Sentinel-2 data
Şekil 3. *Sentinel-2 verisinden üretilmiş dNBR temelli yanma şiddeti haritası*

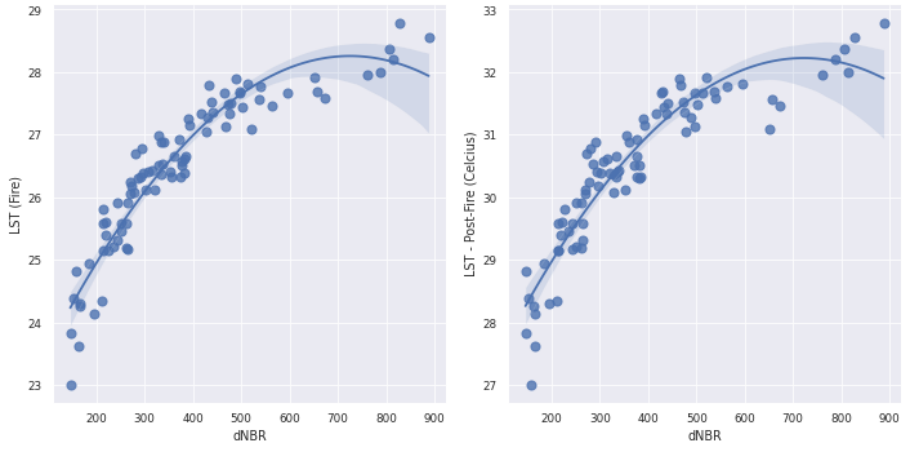

Figure 4. Regression lines between LST and dNBR values
Şekil 4. *LST ve dNBR değerleri arasındaki regresyon çizgileri*

For the pre-fire, fire, and post-fire periods, vertically integrated CO column density maps were created. As illustrated in Figure 5, CO gases travel downwind to the Mediterranean Sea. Despite the fact that CO levels in most pixels near the affected zone reached 0.05 mol/m^2, the CO gas did not move into urban areas and did not cause significant air pollution in the zone. Because the gas died above the sea, the post-fire concentrations are the same as they were before the fire. CO concentrations have a daily average of 0.039 mol/m^2 during the post-fire period, which is very close to pre-fire concentrations (0.035 mol/m^2). During the fire, CO concentrations averaged 0.058 mol/m^2 on a daily basis, peaking at 0.071 mol/m^2 on July 29 near Aydıncık Coast.

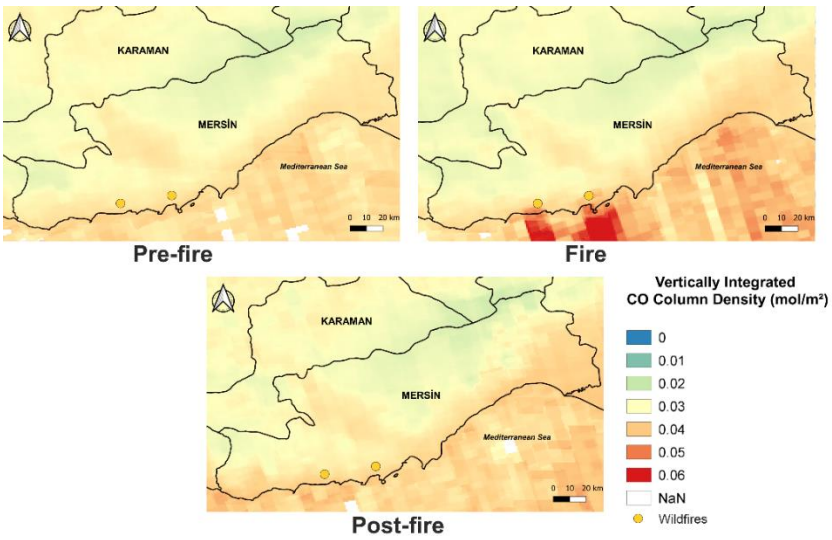

Figure 5. Pre-fire, fire, and post-fire CO maps for Mersin province
Şekil 5. *Mersin ili yangın öncesi, yangın esnasında ve yangın sonrası CO haritaları*

Tropospheric HCHO column number density maps for the pre-fire, fire, and post-fire periods were also created. Figure 6 shows that Mersin Province has a significant amount of high concentrations of HCHO, particularly in industrial areas. The wildfires, on the other hand, released a significant amount of HCHO in the downwind direction towards the sea. During the fire, the daily maximum level of HCHO on the coast of Yeşilovacık village reached 0.0043 mol/m^2 on July 30. Following the wildfire, the HCHO particles followed the wind direction to the west, and there were still high levels of HCHO concentrations (0.0031 mol/m^2) in the western part of the affected area.

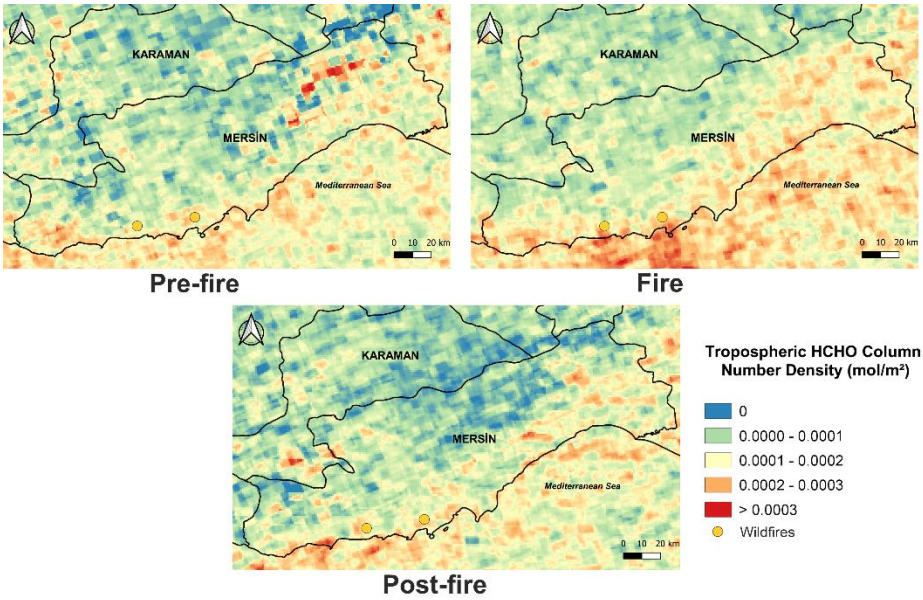

Figure 6. Pre-fire, fire, and post-fire HCHO maps for Mersin province
Şekil 6. *Mersin ili yangın öncesi, yangın esnasında ve yangın sonrası HCHO haritaları*

Figure 7 depicts tropospheric SO_2 column number density maps for the pre-fire, fire, and post-fire periods. On July 30, the maximum amount of SO_2 concentration was measured as 0.00049 mol/m^2 in the Aydıncık district. Vertical columns of SO_2 travel in the same direction as the wind, and are scattered to the north and south of the affected zone. Following the fire, SO_2 concentrations followed the same path as HCHO concentrations, possibly due to the changing direction of the wind, and there was still a lot of SO_2 in the western part of the area. Because the season was dry and non-rainy, higher SO_2 concentrations had no effect on urban areas.

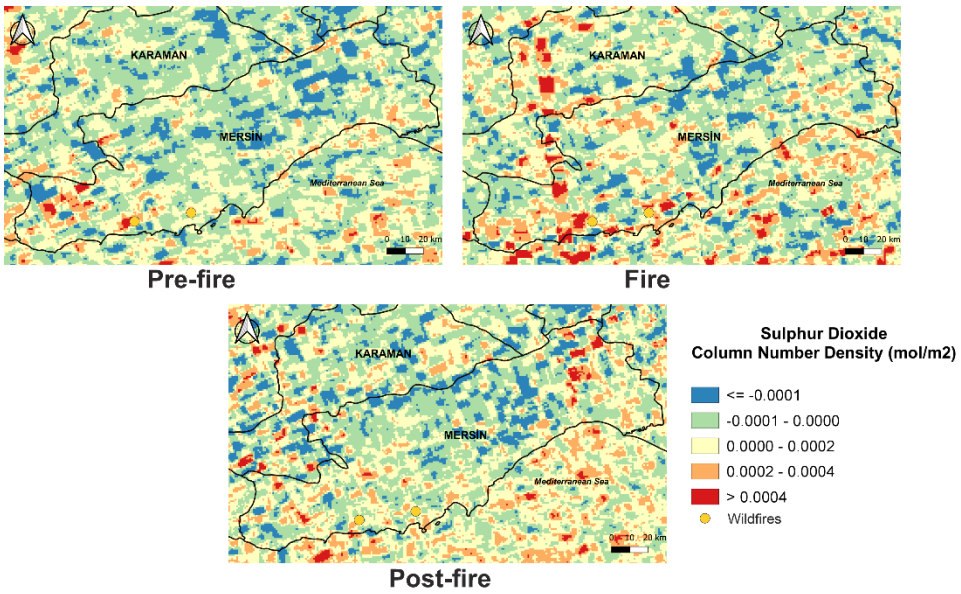

Figure 7. Pre-fire, fire, and post-fire SO_2 maps for Mersin province
Şekil 7. *Mersin ili yangın öncesi, yangın esnasında ve yangın sonrası SO_2 haritaları*

Figure 8 demonstrates that the chemical reactions for O_3 production did not occur instantly during the fire period. Instead, ozone concentrations in tropospheric layers increased even hundreds of kilometres away as a result of NO_x emissions available throughout the province. Because the air is warm and slow after the wildfires, an "ozone episode" occurred in the atmosphere on August 4, with an ozone concentration of 0.137 mol/m^2.

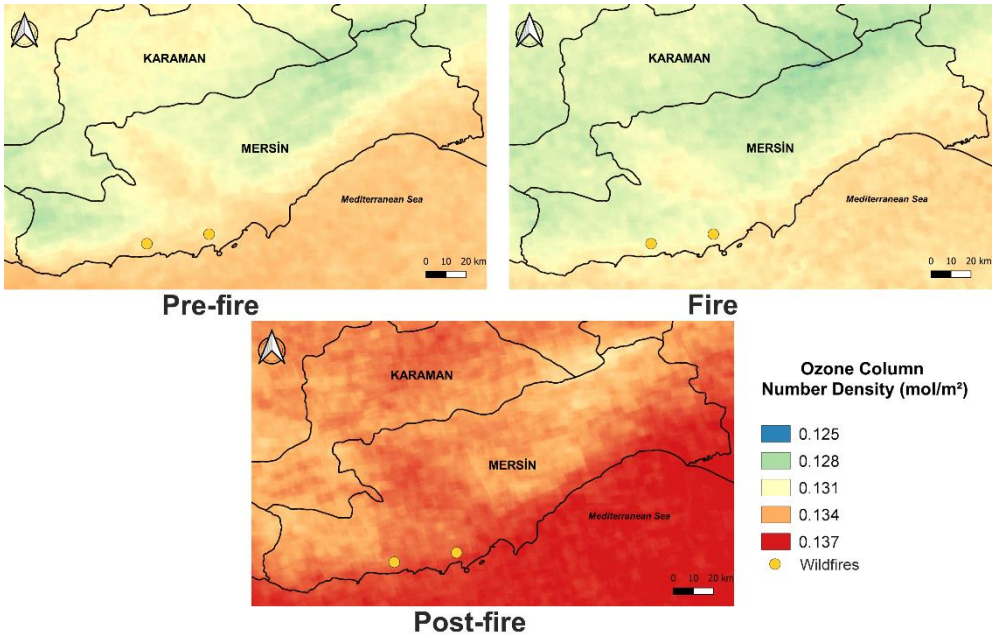

Figure 8. Pre-fire, fire, and post-fire O_3 maps for Mersin province
Şekil 8. *Mersin ili yangın öncesi, yangın esnasında ve yangın sonrası O_3 haritaları*

As a downlooking spectrometer, TROPOMI retrieves Vertical Column Density (VCD), providing researchers with an illustration of the total number of molecules over a vertical slice. A mixing fraction, on the other hand, is often defined in parts per million and is intended to articulate the average number of molecules in a parcel of air. As a result, comparing our results with critical levels of these trace gases requires a conversion from a quantity per area to a quantity in a volume. An atmospheric chemistry model is required to estimate the likely vertical distribution of trace gases in order to make such a comparison. This study aimed to demonstrate the fluctuations of

trace gases in VCDs using TROPOMI data; thus, the current data set used has the limitation of distributing gas concentration levels in different layers of columns. The maps created for this study clearly show that the levels of atmospheric trace gases increased significantly during and after the Mersin wildfire events; however, it is not possible to determine which areas were exposed to concentrations above critical levels.

4. Conclusions
4. Sonuçlar

The land and atmospheric data retrieved from satellite remote sensing platforms were analyzed in this study to determine the burn severity of extreme wildfires in Mersin Province that occurred in the summer of 2021, as well as to visualize the fluctuations of atmospheric trace gases, known to be air pollutants, across the entire province.

The data acquisition chunk of this study supports the idea that Sentinel 2A, 5P TROPOMI and MODIS products are powerful tools for obtaining instantaneous data for the area of interest's terrestrial and atmospheric content. The quantitative results of burn severity work show that there were high and moderately effected zones in the wildfire region, and there has been no improvement in vegetation growth so far. Furthermore, the land surface temperatures and the burn severity are found to be positively correlated. The amount of pollutants in the atmosphere was found to be increasing during and after the extreme wildfire events. The direction of trace gases followed the direction of the wind, and the majority of the gases were captured at sea. It has not been encountered that there was a significant increase in air pollutants near urban areas. However, ozone concentrations increased significantly after the wildfire event because the nitrogen oxide levels in the entire province were sufficient to produce ozone.

Author contribution
Yazar katkısı

MCİ: Literature review, conceptual design, data pre-processing, data visualization, writing and editing. EŞ: data preparation, data processing, data visualization, writing and editing. Both authors read and confirmed the article.

Declaration of ethical code
Etik beyanı

Bu makalenin yazarları, bu çalışmada kullanılan materyal ve yöntemlerin etik kurul izni ve / veya yasal-özel izin gerektirmediğini beyan etmektedir.

Conflicts of interest
Çıkar çatışması beyanı

Yazarlar herhangi bir çıkar çatışması olmadığını beyan eder.

Referances
Kaynaklar

Alvarado, L. M. A., Richter, A., Vrekoussis, M., Hilboll, A., Kalisz Hedegaard, A. B., Schneising, O., & Burrows, J. P. (2020). Unexpected long-range transport of glyoxal and formaldehyde observed from the Copernicus Sentinel-5 Precursor satellite during the 2018 Canadian wildfires. *Atmospheric Chemistry and Physics*, *20*(4), 2057–2072. https://doi.org/10.5194/acp-20-2057-2020

Aryal, R., Kafley, D., Beecham, S., & Morawska, L. (2018). Air Quality in the Sydney Metropolitan Region during the 2013 Blue Mountains Wildfire. *Aerosol and Air Quality Research*, *18*(9), 2420–2432. https://doi.org/10.4209/aaqr.2017.10.0427

Bao, Y., Chen, S., Liu, Q., Xiao, Q. & Cao, C., (2011). Land surface temperature and emissivity retrieval by integrating MODIS data onboard Terra and Aqua satellites. *International Journal of Remote Sensing*, *32*(5), 1449–1469. https://doi.org/10.1080/01431160903559754

Cansler, C. A., & McKenzie, D. (2012). How robust are burn severity ındices when applied in a new region? Evaluation of alternate field-based and remote-sensing methods. *Remote Sensing*, *4*(2), 456–483. https://doi.org/10.3390/rs4020456

Chuvieco, E., & Congalton, R. G. (1989). Application of remote sensing and geographic information systems to forest fire hazard mapping. *Remote Sensing of Environment*, *29*(2), 147–159. https://doi.org/10.1016/0034-4257(89)90023-0

Cocke, A. E., Fulé, P. Z., & Crouse, J. E. (2005). Comparison of burn severity assessments using Differenced Normalized Burn Ratio and ground data. *International Journal of Wildland Fire*, *14*(2), 189. https://doi.org/10.1071/WF04010

Çolak, E., & Sunar, F. (2020). Spatial pattern analysis of post-fire damages in the Menderes District of Turkey. *Frontiers of Earth Science*, *14*(2), 446–461. https://doi.org/10.1007/s11707-019-0786-4

Díaz-Delgado, R., Lloret, F., & Pons, X. (2003). Influence of fire severity on plant regeneration by means of remote sensing imagery. *International*

Journal of Remote Sensing, *24*(8), 1751–1763. https://doi.org/10.1080/01431160210144732

Dindaroglu, T., Babur, E., Yakupoglu, T., Rodrigo-Comino, J., & Cerdà, A. (2021). Evaluation of geomorphometric characteristics and soil properties after a wildfire using Sentinel-2 MSI imagery for future fire-safe forest. *Fire Safety Journal*, *122*, 103318. https://doi.org/10.1016/j.firesaf.2021.103318

Ebrahimy, H., Aghighi, H., Azadbakht, M., Amani, M., Mahdavi, S., & Matkan, A. A. (2021). Downscaling MODIS land surface temperature product using an adaptive random forest regression method and Google Earth Engine for a 19-years spatiotemporal trend analysis over Iran. *IEEE Journal of Selected Topics in Applied Earth Observations and Remote Sensing*, *14*, 2103–2112. https://doi.org/10.1109/JSTARS.2021.3051422

Eva, H., & Lambin, E. F. (2000). Fires and land-cover change in the tropics:a remote sensing analysis at the landscape scale. *Journal of Biogeography*, *27*(3), 765–776. https://doi.org/10.1046/j.1365-2699.2000.00441.x

Fassnacht, F. E., Schmidt-Riese, E., Kattenborn, T., & Hernández, J. (2021). Explaining Sentinel 2-based dNBR and RdNBR variability with reference data from the bird's eye (UAS) perspective. *International Journal of Applied Earth Observation and Geoinformation*, *95*, 102262. https://doi.org/10.1016/j.jag.2020.102262

Fernández, C., Vega, J. A., Fonturbel, T., Pérez-Gorostiaga, P., Jiménez, E., & Madrigal, J. (2007). Effects of wildfire, salvage logging and slash treatments on soil degradation. *Land Degradation & Development*, *18*(6), 591–607. https://doi.org/10.1002/ldr.797

Fu, A. S. (2022). *Risky cities: The physical and fiscal nature of disaster capitalism*. Rutgers University Press.

Imhoff, M. L., Zhang, P., Wolfe, R. E., & Bounoua, L. (2010). Remote sensing of the urban heat island effect across biomes in the continental USA. *Remote Sensing of Environment*, *114*(3), 504–513. https://doi.org/10.1016/j.rse.2009.10.008

Kaplan, G., & Yigit Avdan, Z. (2020). Space-borne air pollution observation from Sentinel-5p TROPOMI: relationship between pollutants, geographical and demographic data. *International Journal of Engineering and Geosciences*, *5*(3), 130-137. https://doi.org/10.26833/ijeg.644089

Keeley, J. E. (2009). Fire intensity, fire severity and burn severity: a brief review and suggested usage. *International Journal of Wildland Fire*, *18*(1), 116. https://doi.org/10.1071/WF07049

Key, C. H., & Benson, N. C. (2006). *Landscape assessment (LA) sampling and analysis methods*.

Langmann, B., Duncan, B., Textor, C., Trentmann, J., & van der Werf, G. R. (2009). Vegetation fire emissions and their impact on air pollution and climate. *Atmospheric Environment*, *43*(1), 107–116. https://doi.org/10.1016/j.atmosenv.2008.09.047

Lindenmayer, D. B., Kooyman, R. M., Taylor, C., Ward, M., & Watson, J. E. M. (2020). Recent Australian wildfires made worse by logging and associated forest management. *Nature Ecology & Evolution*, *4*(7), 898–900. https://doi.org/10.1038/s41559-020-1195-5

Liu, X., Huey, L. G., Yokelson, R. J., Selimovic, V., Simpson, I. J., Müller, M., Jimenez, J. L., Campuzano-Jost, P., Beyersdorf, A. J., Blake, D. R., Butterfield, Z., Choi, Y., Crounse, J. D., Day, D. A., Diskin, G. S., Dubey, M. K., Fortner, E., Hanisco, T. F., Hu, W., … Wolfe, G. M. (2017). Airborne measurements of western U.S. wildfire emissions: Comparison with prescribed burning and air quality implications. *Journal of Geophysical Research: Atmospheres*, *122*(11), 6108–6129. https://doi.org/10.1002/2016JD026315

Llorens, R., Sobrino, J. A., Fernández, C., Fernández-Alonso, J. M., & Vega, J. A. (2021). A methodology to estimate forest fires burned areas and burn severity degrees using Sentinel-2 data. Application to the October 2017 fires in the Iberian Peninsula. *International Journal of Applied Earth Observation and Geoinformation*, *95*, 102243. https://doi.org/10.1016/j.jag.2020.102243

Magro, C., Nunes, L., Gonçalves, O., Neng, N., Nogueira, J., Rego, F., & Vieira, P. (2021). Atmospheric Trends of CO and CH4 from Extreme Wildfires in Portugal Using Sentinel-5P TROPOMI Level-2 Data. *Fire*, *4*(2), 25. https://doi.org/10.3390/fire4020025

McClure, C. D., & Jaffe, D. A. (2018). Investigation of high ozone events due to wildfire smoke in an urban area. *Atmospheric Environment*, *194*, 146–157. https://doi.org/10.1016/j.atmosenv.2018.09.021

Na, K., & Cocker, D. R. (2008). Fine organic particle, formaldehyde, acetaldehyde concentrations under and after the influence of fire activity in the atmosphere of Riverside, California. *Environmental Research*, *108*(1), 7–14. https://doi.org/10.1016/j.envres.2008.04.004

Nasery, S., & Kalkan, K. (2020). Burn area detection and burn severity assessment using Sentinel 2 MSI data: The case of Karabağlar district, İzmir/Turkey. *Turkish Journal of Geosciences*, *1*(2), 72–77.

National Toxicology Program. (2010). *Final report on carcinogens background document for formaldehyde. Report on Carcinogens Background Document for Formaldehyde*. *Access:*. http://www.ncbi.nlm.nih.gov/pubmed/20737003

Omaye, S. T. (2002). Metabolic modulation of carbon monoxide toxicity. *Toxicology*, *180*(2), 139–150. https://doi.org/10.1016/S0300-483X(02)00387-6

Sabuncu, A., & Özener, H. (2019). Uzaktan Algılama Teknikleri ile Yanmış Alanların Tespiti: İzmir Seferihisar Orman Yangını Örneği. *Doğal Afetler ve Çevre Dergisi*, *5*(2), 317–326. https://doi.org/10.21324/dacd.511688

Salman, T., Zia, U.-H., Ayesha, M., Usman, M., & Waseem, A. (2021). Assessment of air quality during worst wildfires in Turkey. *Natural Hazards*. https://doi.org/https://doi.org/10.21203/rs.3.rs-903604/v1

Savenets, M., Osadchyi, V., Oreshchenko, A., & Pysarenko, L. (2020). Air quality changes in Ukraine during the April 2020 wildfire event. *Geographica Pannonica*, *24*(4), 271–284. https://doi.org/10.5937/gp24-27436

Schneising, O., Buchwitz, M., Reuter, M., Bovensmann, H., & Burrows, J. P. (2020). Severe Californian wildfires in November 2018 observed from space: the carbon monoxide perspective. *Atmospheric Chemistry and Physics*, *20*(6), 3317–3332. https://doi.org/10.5194/acp-20-3317-2020

Tonbul, H., Kavzoglu, T., & Kaya, S. (2016). Assessment of fire severity and post-fire regeneration based on topographical features using multitemporal LANDSAT imagery: A case study in Mersin, Turkey. *ISPRS - International Archives of the Photogrammetry, Remote Sensing and Spatial Information Sciences*, *XLI-B8*, 763–769. https://doi.org/10.5194/isprsarchives-XLI-B8-763-2016

TROPOMI. (2021). *Level 2 Products*. Access: http://www.tropomi.eu/data-products/level-2-products

Wan, Z., Zhang, Y., Zhang, Q., & Li, Z.-L. (2004). Quality assessment and validation of the MODIS global land surface temperature. *International Journal of Remote Sensing*, *25*(1), 261–274. https://doi.org/10.1080/0143116031000116417

Wang, M., He, G., Zhang, Z., Wang, G., Wang, Z., Yin, R., Cui, S., Wu, Z., & Cao, X. (2019). A radiance-based split-window algorithm for land surface temperature retrieval: Theory and application to MODIS data. *International Journal of Applied Earth Observation and Geoinformation*, *76*, 204–217. https://doi.org/10.1016/j.jag.2018.11.015

Watson, G. L., Telesca, D., Reid, C. E., Pfister, G. G., & Jerrett, M. (2019). Machine learning models accurately predict ozone exposure during wildfire events. *Environmental Pollution*, *254*, 112792. https://doi.org/10.1016/j.envpol.2019.06.088

Weber, J.-N., Kaufholdt, D., Minner-Meinen, R., Bloem, E., Shahid, A., Rennenberg, H., & Hänsch, R. (2021). Impact of wildfires on SO_2 detoxification mechanisms in leaves of oak and beech trees. *Environmental Pollution*, *272*, 116389. https://doi.org/10.1016/j.envpol.2020.116389

Wolfe, R. E., Nishihama, M., Fleig, A. J., Kuyper, J. A., Roy, D. P., Storey, J. C., & Patt, F. S. (2002). Achieving sub-pixel geolocation accuracy in support of MODIS land science. *Remote Sensing of Environment*, *83*(1–2), 31–49. https://doi.org/10.1016/S0034-4257(02)00085-8

Wu, J., M Winer, A., & Delfino, R J. (2006). Exposure assessment of particulate matter air pollution before, during, and after the 2003 Southern California wildfires. *Atmospheric Environment*, *40*(18), 3333–3348. https://doi.org/10.1016/j.atmosenv.2006.01.056

Zhang, Y., & Cheng, X. (2017). Satellite observation based thermal anomalies detection for 2016 Menyuan MS6.4 earthquake. *2017 IEEE International Geoscience and Remote Sensing Symposium (IGARSS)*, 1930–1933. https://doi.org/10.1109/IGARSS.2017.8127356